Advances in Geosciences

The integration of novel diagnostics techniques for multi-scale monitoring of large civil infrastructures

F. Soldovieri, R. Bernini, I. Catapano, and L. Crocco

Istituto per il Rilevamento Elettromagnetico dell'Ambiente (IREA-CNR) Consiglio Nazionale delle Ricerche, Napoli, Italy
Via Diocleziano 328, 80124 Napoli, Italy

Abstract. In the recent years, structural monitoring of large infrastructures (buildings, dams, bridges) or more generally man-made structures has raised an increased attention due to the growing interest about safety and security issues and risk assessment through early detection. In this framework, aim of the paper is to introduce a new integrated approach which combines two sensing techniques acting on different spatial and temporal scales. The first one is a distributed optic fiber sensor based on the Brillouin scattering phenomenon, which allows a spatially and temporally continuous monitoring of the structure with a "low" spatial resolution (meter). The second technique is based on the use of Ground Penetrating Radar (GPR), which can provide detailed images of the inner status of the structure (with a spatial resolution less then tens centimetres), but does not allow a temporal continuous monitoring. The paper describes the features of these two techniques and provides experimental results concerning preliminary test cases.

1 Introduction

In civil engineering significant attention is devoted to ensure the safety of structures. Property and condition assessment are key ingredients in the process of evaluating and monitoring the integrity of civil structures (monuments, buildings, etc.) for continued use, change of use, or as a basis for safety evaluation, retrofit or replacement. As the infrastructures age, condition assessment for safety considerations becomes increasingly important. In particular, early detection of objects such as huge structures, long bridges or steep slopes might save thousands of lives because it alerts people prior to the fatal hit of a public disaster.

As a consequence, monitoring technology is a key countermeasure to the natural disaster prevention and the structural health examination for existing structures is one of the main goals. Similarly, safety management of dams for effective maintenance and rehabilitation is also worth to be recalled, as upgrades and reconstruction of dykes and dams are of vital importance to governments, utilities, industry and the general public. As a matter of fact, the importance of dam safety concern the environmental protection, the agriculture, the hydro-power generation and other industries that require large supplies of water.

For many years maintenance of infrastructures has been performed by exploiting patrolling and inspections with an obvious waste of time and resources. For this reason, in the recent years, remote and non invasive observation technology has gained an increasing attention from a maintenance viewpoint, as it would allow to reducing maintenance costs and assuring safety. In addition, this technology improves the efficiency of inspections and allows to continuously observe the physical properties of structures (such as stress, strain and acceleration). Moreover, by means of an off-line analysis of measured data, one can state whether or not repairs, reinforcement or replacement are necessary.

However, a proper management of large civil infrastructures, such as buildings, dams, bridges and road viaducts, is still a challenging aim for the non invasive technologies. As a matter of fact, this kind of structural monitoring entails an accurate knowledge of their inner status, i.e., it requires qualitative (and possibly quantitative) information concerning the extent and the properties of a possible damage. Also, a description of the time-behaviour of the deterioration is convenient. Finally, besides a large scale and possibly remote monitoring, it often needs to provide detailed information on possible anomalies by means of an in situ inspection.

Nowadays, several non invasive diagnostics techniques have been developed ranging from X-ray and gamma-ray radiography to infrared thermography and microwave

Correspondence to: F. Soldovieri
(soldovieri.f@irea.cnr.it)

tomography, only to mention few examples (Buyukizturk, 1998). However, despite the specific positive aspects of each strategy, the very broad requirements raised by large structure monitoring makes it impossible to accomplish the diagnostic task by means of a single kind of sensor. As a consequence, the integration of different technologies appears to be a crucial step towards the development of a diagnostic tool able to provide temporal continuous and detailed assessment on the infrastructures status.

According to the above framework, the proposed idea is to apply two in situ electromagnetic techniques, which are jointly exploited to provide information on a global and a local scale.

The first sensing technique uses distributed optic fiber sensors based on Brillouin scattering phenomenon (Bao et al., 1995; Bernini et al., 2003; Bernini et al., 2005; Bernini et al., 2006) and it allows the remote and spatially continuous monitoring of a structure in terms of temperature and strain. With respect to state-of-the-art settings, innovative measurement methodologies and reconstruction algorithms, that process frequency domain data and reach a spatial resolution of some meters (Bernini et al., 2002; Bernini et al., 2003), are adopted in order to overcome some difficulties of the classical techniques, which are based on time-domain measurement (Bao et al., 1995).

The second technique is based on the use of Ground Penetrating Radar (GPR) (Daniels, 1996) and can provide detailed images of the inner status of the structure under test, with a resolution that can be up to tens of centimetres. In this framework, the research activity is aimed at developing innovative data processing techniques able to give a tomographic image of a section of the inner of the probed structure (Crocco and Soldovieri, 2003; Catapano et al., 2004; Persico et al. 2005; Soldovieri et al. 2007; Piscitelli et al., 2007).

The two techniques can be co-operatively applied in order to ensure a multi-temporal and a multi-spatial scale damage detection of infrastructures, for example bridges and galleries.

In particular, the fiber optic sensors can be permanently installed on the structure and used to realize a wide spread and temporal continuous monitoring. By processing the data provided by these sensors, a low resolution (of the order of the meter) detection of possibly critical anomaly is achieved. Therefore, the GPR tomography is performed on the detected risk area to provide a high resolution image of the inner of the structure. By doing so, the geometrical features of the embedded defects in terms of detection, localization, sizing and, possibly, shaping can be reconstructed. Therefore, the resulting integrated technique can lead to a wide-spread but potentially detailed diagnosis of the infrastructures. To this end, two separate data sets are collected, one by means of the optic fiber sensors and the other one by using GPR, and they are independently processed.

The paper is organised as follows. The fiber optic sensor technique is detailed in Sect. 2, wherein an its experimental validation is also proposed. In Sect. 3, GPR approach is described and experimental results from realistic and controlled test cases are presented. Conclusion follows.

2   The distributed fiber optic sensor

2.1   The formulation of the approach

In the last few years distributed optical fiber sensors have gained an important role because they allow to measure physical quantities like temperature and/or strain over kilometric ranges with high spatial resolution. In particular, distributed sensors based on stimulated Brillouin scattering (SBS) are very promising tools for temperature and/or strain monitoring (Bao et al., 1995; Bernini et al., 2002; Bernini et al., 2003). These sensors are based on the interaction, along an optical fiber, between two counter propagating light waves with frequency shift ν and an acoustic wave of frequency ν. In this three-wave mixing process power is transferred from the pump light wave to the Stokes light wave (that is the light wave having a lower frequency) and also to the acoustic wave. The coupling between the two optical waves occurs due to Bragg diffraction of the light from the refractive index perturbation produced by the acoustic field. The interaction process is described by the Brillouin gain coefficient $g(\nu)$, which depends on the frequency shift ν and attains its maximum at the so called Brillouin frequency shift ν_B. As the Brillouin frequency shift changes linearly with temperature and strain, a distributed temperature-strain sensor can be realized using stimulated Brillouin scattering.

Usually the SBS-based sensing methods work in the time domain (Bao et al., 1995). In this configuration, called Brillouin optical-fiber time domain analysis (BOTDA), the spatial resolution is achieved by using a short pulse and a continuous wave (CW). For these techniques, the temperature-strain reconstruction is achieved by determining the Brillouin shift distribution along the fibre $\nu_B(z)$ by a spectroscopic approach. This is performed by measuring the intensity of the transmitted CW field corresponding to different frequency shifts ν between the two beams as a function of the time, as in Optical-fiber Time Domain Reflectometry. For each section along the fiber, the Brillouin frequency shift is evaluated as the pump-probe frequency difference at which the maximum amplification or depletion of the transmitted CW field occurs.

However, this reconstruction technique suffers from some systematic errors that become relevant as long as the sensing length and/or the CW power increase. In fact, this approach relies on the assumption that a linear relationship exists, at each fiber section, between the Brillouin gain coefficient and measured Brillouin signal. However, the power transfer at each section between the pulse and CW wave, that leads to

the Brillouin signal, also leads to a change of the pulse power that, typically, is not accounted for. Then, the Brillouin signal arising from a certain location along the fiber depends not only on Brillouin gain coefficient in that section, but also on the Brillouin interaction arising at every point between the input and the current measurement point, via the pulse power. As a consequence, the local measurement is affected by non-local effects that limit the sensor performance with the result that long-range and high power level measurements can lead to inaccurate strain and/or temperature determination. In addition, the classical spectroscopic approach also suffers from cross-talk problems, which result in a further distortion of the spectral shape to be analyzed (Geinitz et al., 1999) .

An alternative approach is the frequency domain method (Garus et al., 1997), called Brillouin Optical-fiber Frequency Domain Analysis (BOFDA), where a modulated wave interacts with a continuous one so to obtain the base-band transfer function of the fiber. Such an approach permits an improvement of the signal-to-noise-ratio, but it is still subject to non-local effects. In fact, despite the frequency-domain measurement, the data processing is typically still performed in the time domain after an inverse Fourier transform of the measured data (Garus et al., 1997), in order to extract the local Brillouin gain spectra as occurring in time-domain approaches.

Recently, a novel approach to distributed fiber-optic Brillouin sensing, which is based on measurements and data analysis performed in the frequency domain has been developed (Bernini et al., 2002; Bernini et al., 2003; Bernini et al., 2005; Bernini et al., 2006).

This approach uses an approximated integral equation that directly relates the Brillouin gain $g(z)$ along the optic fiber, whose length is L, to the Brillouin signal $I_p(L,\omega)$, in order to develop an iterative algorithm that allows the reconstruction of the temperature-strain profile along the optical fiber (Bernini et al., 2002; Bernini et al., 2003).

Let $I_{p0}(z)$ be the intensity of the CW wave and $I_{s0}(z)$ that of the modulated waves (Stokes wave), which are the steady-state solutions of the two coupled equations describing the Brillouin scattering. The approximated integral equation is given by:

$$I_p(L,\omega) = -I_{m1}\exp\left[-2\left(j\frac{\omega}{v}+\alpha\right)L\right]$$

$$\times \int_0^L g(z'')I_{p0}(z'')\exp\left[\int_{z''}^L g(z')\left[I_{p0}(z')-I_{s0}(z')\right]dz'\right]$$

$$\exp\left[2\left(j\frac{\omega}{v}+\alpha\right)z''\right]dz'' \qquad (1)$$

where α is the fiber loss coefficient, and v is the velocity of the light wave in the fiber.

The proposed algorithm is based on the expansion of the unknown Brillouin frequency shift profile by using a suitable space of base functions and searching for an its representation, which minimize a cost-function defined as the square
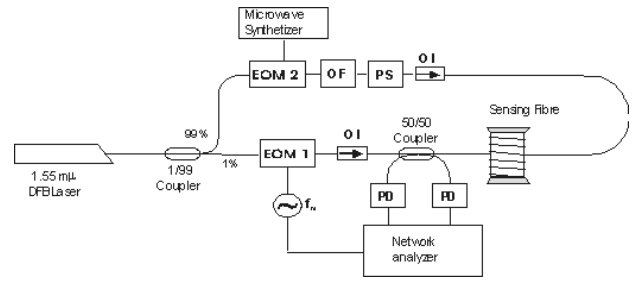

Fig. 1. Experimental setup for Brillouin Optical Frequency-domain analysis.

norm, in the ω space, of the difference between the measured and the model signals (Bernini et al., 2002; Bernini et al., 2003).

Numerical results show that this approach is able to compensate for the systematic errors suffered by the spectroscopic approaches.

2.2 The experimental results

In this Section, we verify the performances of the above approach in the framework of strain detection by processing experimental data collected in a controlled condition. Measurements were performed in order to validate this novel harmonic reconstruction technique. To this aim, the experimental configuration shown in Fig. 1 was employed. The semiconductor laser was a pigtailed DFB module emitting at $1.550\,\mu$m with an output power of about 40 mW. The output light was first split by a fiber-fused coupler, which directed the 1% of the power to a first electro-optic modulator (EOM1) for the AC-modulated pump signal generation, whereas the remaining 99% was launched into a second high-bandwidth electro-optic modulator (EOM2). This latter was employed for the generation of a CW light having an opportune frequency offset (about10 GHz), by means of the sideband technique. A pass-band optical filter (OF) is placed after the EOM in order to suppress one of the two generated sidebands. The polarization scrambler (PS) is used in order to eliminate the Brillouin gain fluctuations due to changes in the state of polarization (SOP) of the two beams occurring along the fiber. The measured input optical powers are P_{P0_0}=1 mW and P_{S0_L}=30 μW. Measurements were taken by making use of a modulation frequency ranging from 40 KHz to 250 MHz. For each measurement, we compare the reconstruction provided by the harmonic approach with the one achieved by local fitting of the Brillouin gain spectrum at each section along the fiber. In the latter case, Brillouin gain spectra are extracted by inverse-Fourier-transform of the frequency-domain data.

The optical fiber acting as the sensor head was a standard single-mode fiber, with a jacket diameter of 900 μm and a total length of 10 m. A strand of fiber was glued to

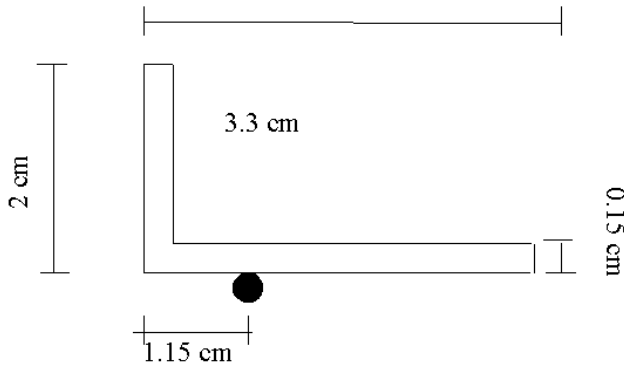**Fig. 2.** Cross section of the aluminum beam used for the experiments.

Fig. 3. Axial strain profile along the beam at the fiber position. The concentrated load was $P=1000$ g (solid line=numerical, circles=experimental), and $P=500$ g (dotted line=numerical, triangles=experimental).

a 2.96 m-long L-shaped aluminium beam, along an axial line of the beam. The cross-section of the beam, as well as the position of the optical fiber sensor, are shown in Fig. 2.

A perfect adherence between the fiber and the beam is supposed, so that the axial strain distribution measured along the fiber gives a quantitative picture of the deformation of the beam under test, at the positions where the fiber is glued. The beam structure has been also modelled by FEM simulations, the Young modulus of the aluminium being set to 60 GPa.

A concentrated load was applied at the centre of the beam, by means of a fixed weight.

The measured axial strain profiles, together with the corresponding FEM simulations, are shown in Fig. 3 for an applied weight of 500 g, and 1000 g. As it can be seen, an overall qualitative agreement is found between the measured and the numerically evaluated strain profiles.

3 The ground penetrating radar

3.1 The approach

The GPR technology has gained an increasing interest in various applicative fields, ranging from archaeological prospecting to geophysical exploration, from monitoring of industrial items to demining, only to quote few examples (Daniels, 1996).

Usually, GPR works by generating and radiating several short pulses (pulsed GPR) or, alternatively, several time harmonic waves (stepped frequency GPR) towards a medium that hosts the target medium. When the transmitted wave hits an object with different electromagnetic properties (dielectric permittivity, conductivity) respect to the hosting medium a backscattered electromagnetic wave arises that is recorded at a receiving antenna. Since a field embeds information about the electromagnetic properties of the object, suitable processing can lead to reveal the presence and the location of the target as well as to characterize its properties. The acquisition setup is usually bistatic, i.e. the transmitter and the receiver
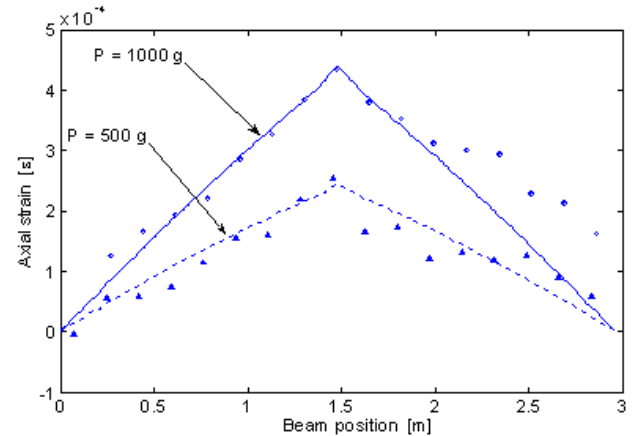
are spaced by a fixed offset, possibly equal to zero if the same antenna is exploited as transmitter and receiver (in this case we have a monostatic configuration).

The data are obtained by moving the antennas along the air-medium interface and, in its customary modality of use, GPR provides a radargram that is the image of the echoes reflected by the embedded scattering objects.

However, a difficulty arises in interpreting the radargram in order to work out the presence and the location of the embedded targets. As a matter of fact, such interpretation is strongly dependent on the user's expertise. Thus, the need to develop processing techniques able to provide a "clear" radargram (thus reducing as much as possible the dependence from a subjective interpretation) arises.

On the other hand, although GPR works in principle as a traditional radar system, usually adopted radar signal processing techniques cannot be applied in a straightforward fashion. As a matter of fact, unlike traditional radar systems, the transmitted and backscattered waves travel in a medium which is only partially known and the targets are often located in the near field respect to the probes. As a consequence, standard radar procedures cannot immediately applied and suitable processing techniques have to be developed.

In the last few years, among the different developed techniques, tomographic approaches have been gained interest (Daniels, 1996; Lesselier and Duchene, 1996; Catapano et al., 2004; Persico et al., 2005, Soldovieri et al., 2007).

These approaches are based on the solution of an inverse scattering problem and are able to provide a spatial map of the dielectric permittivity and/or of the electrical conductivity of a subsurface region. This permits to achieve information not only about the presence and the position of the object but possibly also about its extent and shape.

On the other hand, to face a full inverse scattering problem without any approximation entails serious mathematical difficulties due to its inherent ill-posedness and nonlinearity and it leads to computationally intensive solution algorithms, which are often not affordable from a practical point of view.

A convenient way to afford this kind of problem is to adopt approximate models to describe the electromagnetic scattering. In this paper we assume a linear model provided by the Born Approximation (BA) that holds for penetrable objects (Lesselier and Duchene, 1996; Persico et al., 2005; Soldovieri et al., 2007). The adoption of the linear model allows to set up efficient processing algorithms able to deal with electrically large investigation domain in "quasi-real time". Another important advantage in using a linear model consists in the possibility to exploit powerful mathematical tools, as the Singular Value Decomposition (SVD) (Bertero and Boccacci, 1998) which allows to achieve a stable solution of the problem and provides an insight about the ultimate performances of the inversion scheme (Persico et al., 2005). This latter analysis is of interest since it provides useful guidelines to choice the measurement parameters and to foresee the reconstruction capabilities of the inversion algorithm in terms of resolution limits.

In order to set up the tomographic inversion procedure, the problem can be conveniently modelled considering the air-medium interface as the planar interface separating two half-spaces (at $z=0$); the upper half space being the air, while the lower one schematizing a homogeneous medium with relative dielectric permittivity ε_b and conductivity σ_b. For sake of simplicity a 2-D geometry is considered. Therefore, the cross-section of the hidden objects is supposed to be invariant along the y-axis and enclosed in a rectangular investigation domain $D=[-a, a] \times [z_{\min}, z_{\min} + 2b]$. The unknowns of the problem are the relative dielectric permittivity $\varepsilon_D(x, z)$ and the conductivity $\sigma_D(x, z)$ functions inside D. The source of the incident field (E_{inc}) is supposed to be a time-harmonic (time dependence $\exp(j\omega t)$, $\omega=2\pi f$) filamentary y-directed electric current (TM-polarization), of infinite extent and invariant along the y-axis. Therefore, the problem at hand is 2-D and scalar.

The source is moved along the interface (at $z=0$) into various abscissas x_s within the interval $\Sigma = [-x_M, x_M]$. The electric field scattered by the buried objects is measured along the interface at the observation point x_o varying also within Σ.

Under the above assumptions and within the BA, the unknown-data relationship for each frequency in the range $[f_{\min}, f_{\max}]$ is provided by the following equation

$$E_s(x_s, x_o, \omega) =$$
$$k_s^2 \int_D G_e(x_o, \omega, \boldsymbol{r'}) E_{\text{inc}}(x_s, \omega, \boldsymbol{r'}) \chi(\omega, \boldsymbol{r'}) d\boldsymbol{r'} \quad (2)$$

where E_s denotes the scattered electric field probed at x_o when the source is located at x_s; k_s is the wavenumber in the lower half space; k_o indicates the wavenumber in the upper

half space, G_e the (known) Green's function and the "contrast" function χ being defined as:

$$\chi(x', z', \omega) = \frac{\varepsilon_{eq}(x', z', \omega) - \varepsilon_{eqb}(\omega)}{\varepsilon_{eqb}(\omega)} \quad (3)$$

where $\varepsilon_{eq}(x', z', \omega) = \varepsilon_0 \varepsilon_D(x', z', \omega) - j\frac{\sigma_D(x', z')}{\omega\varepsilon_0}$ and $\varepsilon_{eqb}(\omega) = \varepsilon_0 \varepsilon_b - j\frac{\sigma_b}{\omega\varepsilon_0}$.

In order to express the mathematical relationship between the contrast and the data within a multibistatic configuration, we particularize Eq. (2) to the case $x_o=x_s + \Delta$, being Δ the fixed offset (clearly, $\Delta=0$ describes the multimonostatic case). Moreover, to numerically solve the problem, the integral equation Eq. (2) is discretized by exploiting the Method of Moments with a point matching. In particular, the basis function exploited to represent the contrast function are Fourier harmonics along the horizontal direction and rectangular pulses along the depth. By doing so, the problem to be solved is stated as:

$$\boldsymbol{E}_s = A[\boldsymbol{\chi}] \quad (4)$$

wherein $\boldsymbol{E}_s$ is the data matrix, $\boldsymbol{\chi}$ is the vector of the unknown coefficients and the matrix A is the discrete representation of the operator linking data and unknowns. The solution of this problem is achieved by means of the SVD tool.

The SVD of the matrix A, provides the singular system $\{\sigma_n, u_n, v_n\}_{n=0}^{\infty}$ (Bertero and Boccacci, 2005), where the set $\{\sigma_n\}_{n=0}^{\infty}$ denotes the sequence of the singular values ordered in a non increasing sequence and u_n and v_n form the basis for the space of the visible objects (i.e., the objects that could be retrieved by the error-free data) and for the closure of the range of the operator (that is the space of the noise-free data within the BA model), respectively. In this framework, the ill-posedness of the problem can be faced by exploiting the Truncated SVD expansion (TSVD). In particular, by restricting the solution space to that spanned by the first N singular functions u_n, the solution is given by:

$$\boldsymbol{\chi} = \sum_{n=0}^{N} \frac{1}{\sigma_n} < \boldsymbol{E}_s, v_n > u_n. \quad (5)$$

By doing so, the effect of errors on data is not amplified and a stable solution is achieved. The choice of the index N depends on the amount of noise affecting the data and it is performed by taking into account the "degree of regularization" one wants to apply in the inversion in order to obtain a stable solution.

3.2 The experimental results

To show the features of the inverse scattering approach as compared to traditional radar techniques, as first example we show the processing of a set of experimental multi-monostatic data (i.e. $\Delta=0$), which have been gathered (in time domain) in Switzerland on a bridge 25m long, with an
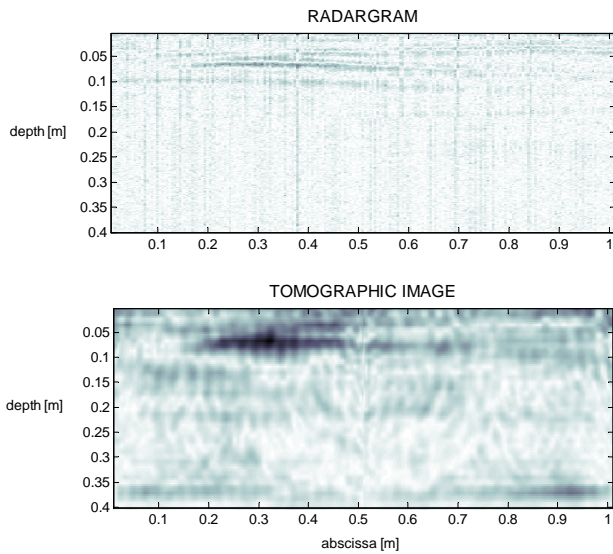
Fig. 4. Comparison between the radargram and the tomographic reconstruction for bridge inspection.

Fig. 5. Cavity buried in a bricks wall: radargrams related to six parallel measurement lines at different heights.

antenna with central frequency equal to 1.4 GHz and nominal band equal to 2.5 GHz. Backscattered field data have been extracted from raw data by gating in time domain the contributions of the direct coupling between the antennas and that of the interface. After temporal gating, data in frequency domain have been obtained by Fourier transforming the gated temporal data. The exploited band ranges from 300 MHz to 2.5 GHz, and the chosen frequency step is equal to 100 MHz. The whole point was investigated and Fig. 4 depicts the tomographic reconstruction compared to the classical radargram for an observation line 1 m long. The regularized inversion is performed by means of the TSVD. In particular, we discarded in the SVD expansion those singular values whose magnitude is lower than –20 dB with respect to that of the first one. Both the radargram and the tomographic image show that some electromagnetic anomalies are present for a depth ranging from 0.05 m and 0.1 m and an abscissa which is between 0.2 m and 0.5 m. However, the tomographic image is more clear and accurate than the radargram and it allows to give indication of the possible presence of a layer of rebars at a depth of about 0.075 m.

As a second example, let us consider an experimental data set concerning the monitoring of a bricks wall 0.24 m thick, 1.49 m high and 1 m large. A cavity (0.50 m×0.20 m×0.12 m) is hidden in the wall at 0.80 m from the floor. The measurement region is a rectangular grid of size 0.89 m 0.76 m and the data have been collected at 11 frequencies, uniformly spaced in the range 0.5–1.5 GHz, by using a multibistatic configuration. In particular, the probes are moved along 21 lines parallel to the floor and, for any fixed quote z, the transmitting antenna is moved in 15 points along a line of 0.6 m with a spatial step of 0.04 m. The offset
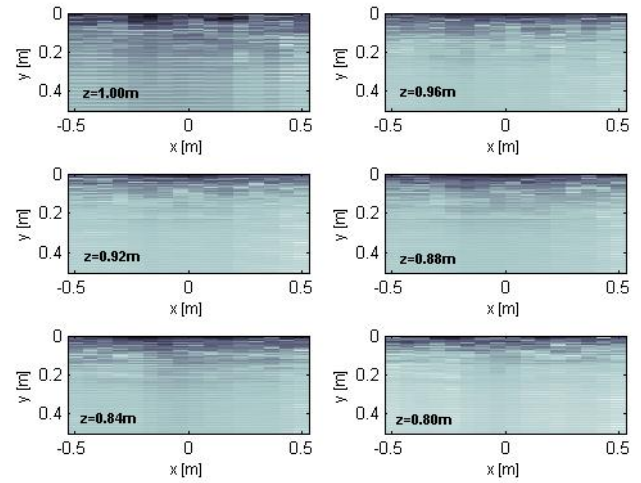
between transmitting and receiving antennas is 0.16 m. As in the previous example, backscattered field data have been extracted from raw data by gating in time domain. To this end, time domain data have been obtained by means an inverse Fourier transform and, after the time gating procedure, they have been retransformed in the frequency domain. Figure 5 shows the raw-data for six parallel measurement lines, each one corresponding to a fixed value of z ranging from 0.8 m to 1.0 m. Looking to this figure it is a hardly work to detect and localize the cavity. This last is, instead, clearly retrieved by applying the tomographic approach as shown in Fig. 6, which provide a satisfactory geometrical characterization. It is worth to note that a good reconstruction is achieved as long as the measurement line corresponds to the central part of the cavity, while the quality of the result downgrades when the measurement line is moved towards the upper and lower edges of the cavity. This behaviour is due to the model error. As a matter of fact, notwithstanding the cavity is a 3-D objects whose size in each spatial direction is comparable to the wavelength, a 2-D scalar model has been adopted in the inversion procedure, which is carried out by using the TSVD. Also in this case, singular values whose magnitude is lower than –20 dB with respect to that of the first one have been cut.

4 Conclusions

As far as infrastructure monitoring is concerned, the cooperative use of different diagnostic tools appears to be a convenient way to overcome the limits of each single approach and develop an integrated system, which should be able to satisfy the required constrains in terms of temporal and spatial resolution.

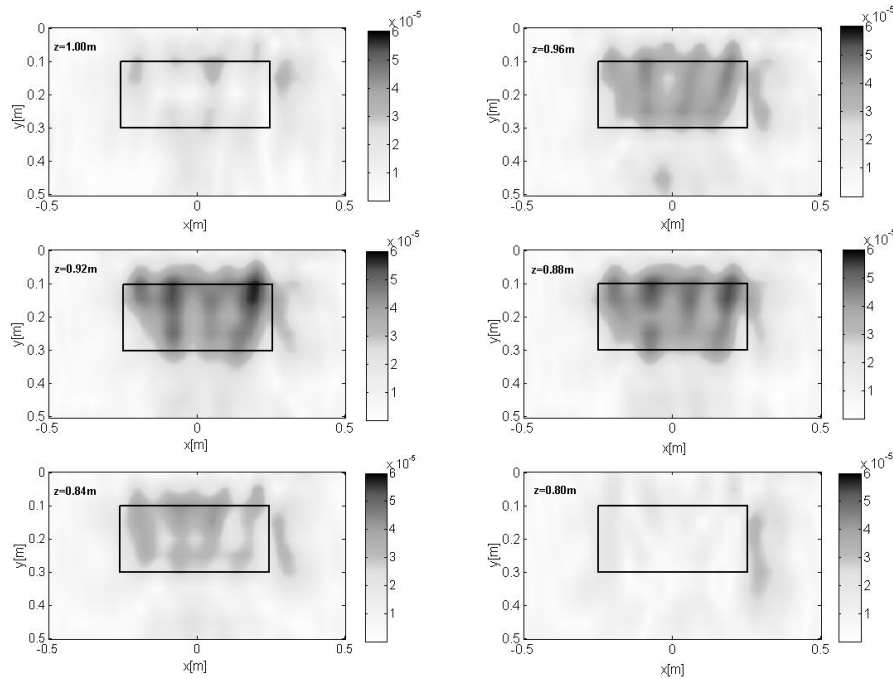In order to pursue this aim, the proposed strategy aims at exploiting distributed fiber optic sensors and GPR

Fig. 6. Tomographic reconstruction of a cavity buried in a bricks wall at different heights. The black line denotes the cavity contour.

technology in a two steps strategy, where the fiber optic sensors are used to constantly monitoring the structure and detect risk areas and then the GPR analysis is performed on these regions to provide a high resolution image of the inner status and then to characterize the electromagnetic anomalies. In particular, as far as fiber optic sensors are concerned, innovative detection and reconstruction techniques have been explored, which are based on the Brillouin scattering in frequency domain instead of time one. On the other hand, the performances of GPR investigation have been improved by considering, instead of classical radargrams in time domain, tomographic images. These last have been obtained by processing the GPR data in the frequency domain by means of a linear inverse scattering approach based on the Born approximation.

The joint use of the above electromagnetic techniques provides an in situ diagnostic tool, which should allow a continuous monitoring of large structures both in time and in space, while at same time it should provide a detailed diagnosis of the defects in terms of their geometrical features. Since in the integrated approach two distinct data sets are collected and independently processed, a preliminary proof of the effectiveness of the monitoring tool has been given by assessing the reconstructions capabilities of each single technique against experimental data. However, further validations on common test sites are necessary and they will be matter of our future work.

References

Bao, X., Dhiliwayo, J., Heron, N., Webb, D. J., and Jackson, D. A.: Experimental and theoretical studies on a distributed temperature sensor based on Brillouin scattering, J. Lightwave Technol., 13(7), 1340–1348, 1995.

Bernini, R., Crocco, L., Minardo, A., Soldovieri, F., and Zeni, L.,: A new frequency domain approach to distributed fiber-optic Brillouin sensing, Opt. Lett., 27(5), 288–290, 2002.

Bernini, R., Crocco, L., Minardo, A., Soldovieri, F., and Zeni, L.: All frequency domain distributed fiber-optic Brillouin sensing, IEEE Sensors Journal, 3(1), 36–43, 2003.

Bernini R., Fraldi M., Minardo A., Minutolo V., Carannante F., Nunziante L., and Zeni, L.: Optical fiber-sensor measurements for safety assessment and monitoring of bridges and large structures, Bridge Structures, 1(3), 355–363, 2005.

Bernini R., Fraldi M., Minardo A., Minutolo V., Carannante F., Nunziante L., and Zeni L.: Identification of Defects and Strain Error Estimation in Bending Steel Beams Through Time-Domain Brillouin Distributed Optical Fiber Sensors, Journal of Smart Materials and Structures, 15, 612–622, 2006.

Bertero, M. and Boccacci, P.: Introduction to Inverse Problems in Imaging, Institute of Physics Publishing, Bristol and Philadelphia, 1998.

Buyukizturk, O.: Imaging of concrete structures, NDT&E International, 31, 233–243, 1998.

Catapano, I., Crocco, L., and Isernia, T.: A simple two-dimensional inversion technique for imaging homogeneous targets in stratified media, Radio Science, 39, RS1012, doi:10.1029/2003RS002917, 2004.

Crocco, L. and Soldovieri, F.: GPR prospecting in a layered medium via microwave tomography, Ann. Geophys., 46(3), 559–572, 2003.

Daniels, J.: Subsurface Penetrating Radar, The Institution of Electrical Engineers, London, UK, 1996.

Garus, D., Gogolla, T., Krebber, K., and Schliep, F.: Brillouin optical-fiber frequency-domain analysis for distributed temperature and strain measurements, J. Lightwave Technol., 15(4), 654–662, 1997.

Geinitz, E., Jetshke, S., Röpke, U., Schröter, S., Willsch, R. and Bartelt, H.: The influence of pulse amplification on distributed fibre-optic Brillouin sensing and a method to compensate for systematic errors, Meas. Sci. Technol., 10, 112–116, 1999.

Lesselier, D. and Duchene, B.: Wavefield inversion of objects in stratified environments, From backpropagation schemes to full solution, Review of Radio Science 1993–1996, edited by: Stone, R., Oxford: Oxford University Press, 235–268, 1996.

Persico, R., Bernini, R., and Soldovieri, F.: The role of the measurement configuration in inverse scattering from buried objects under the Born approximation, IEEE Trans. Antennas and Propagation, 53(6), 1875–1887, June 2005.

Piscitelli S., Rizzo E., Cristallo F., Lapenna V., Crocco L., Persico R., and Soldovieri F.: GPR and microwave tomography for detecting shallow cavities in the historical area of Sassi of Matera (Southern Italy), Near Surface Geophysics, 5(4), 275–284, August 2007.

Soldovieri F., Hugenschmidt J., Persico R., Leone G.: A linear inverse scattering algorithm for realistic GPR applications, Near Surface Geophysics, vol. 5, no. 1, pp. 29-42, February 2007.